

## A Comparative Study between Evaluation Methods for Quality Control Procedures for Determining the Accuracy of PET/CT Registration

Min Kyoung CHA

*Department of Biomedical Engineering, Research Institute of Biomedical Engineering,  
College of Medicine, the Catholic University of Korea, Seoul 137-040, Korea and  
Department of Nuclear Medicine, Asan Medical Center, Seoul 138-736, Korea*

Hyun Soo KO and Woo Young JUNG

*Department of Nuclear Medicine, Asan Medical Center, Seoul 138-736, Korea*

Jae Kwang RYU

*Department of Nuclear Medicine, Asan Medical Center,  
Seoul 138-736, Korea, and Department of Environmental Health,  
Graduate School of Public Health, Seoul National University, Seoul 151-015, Korea*

Bo-Young CHOE\*

*Department of Biomedical Engineering, Research Institute of Biomedical Engineering,  
College of Medicine, the Catholic University of Korea, Seoul 137-040, Korea*

(Received 6 February 2015, in final form 6 March 2015)

The Accuracy of registration between positron emission tomography (PET) and computed tomography (CT) images is one of the important factors for reliable diagnosis in PET/CT examinations. Although quality control (QC) for checking alignment of PET and CT images should be performed periodically, the procedures have not been fully established. The aim of this study is to determine optimal quality control (QC) procedures that can be performed at the user level to ensure the accuracy of PET/CT registration. Two phantoms were used to carry out this study: the American college of Radiology (ACR)-approved PET phantom and National Electrical Manufacturers Association (NEMA) International Electrotechnical Commission (IEC) body phantom, containing fillable spheres. All PET/CT images were acquired on a Biograph TruePoint 40 PET/CT scanner using routine protocols. To measure registration error, the spatial coordinates of the estimated centers of the target slice (spheres) was calculated independently for the PET and the CT images in two ways. We compared the images from the ACR-approved PET phantom to that from the NEMA IEC body phantom. Also, we measured the total time required from phantom preparation to image analysis. The first analysis method showed a total difference of  $0.636 \pm 0.11$  mm for the largest hot sphere and  $0.198 \pm 0.09$  mm for the largest cold sphere in the case of the ACR-approved PET phantom. In the NEMA IEC body phantom, the total difference was  $3.720 \pm 0.97$  mm for the largest hot sphere and  $4.800 \pm 0.85$  mm for the largest cold sphere. The second analysis method showed that the differences in the x location at the line profile of the lesion on PET and CT were (1.33, 1.33) mm for a bone lesion, (-1.26, -1.33) mm for an air lesion and (-1.67, -1.60) mm for a hot sphere lesion for the ACR-approved PET phantom. For the NEMA IEC body phantom, the differences in the x location at the line profile of the lesion on PET and CT were (-1.33, 4.00) mm for the air lesion and (1.33, -1.29) mm for a hot sphere lesion. These registration errors from this study were reasonable compared to the errors reported in previous studies. Meanwhile, the total time required from phantom preparation was  $67.72 \pm 4.50$  min for the ACR-approved PET phantom and  $96.78 \pm 8.50$  min for the NEMA IEC body phantom. When the registration errors and the lead times are considered, the method using the ACR-approved PET phantom was more practical and useful than the method using the NEMA IEC body phantom.

PACS numbers: 87.56.Fc, 87.58.Fg, 87.57.Gg

Keywords: PET/CT, Registration, Accuracy, Quality control

DOI: 10.3938/jkps.67.574

## I. INTRODUCTION

Combined positron emission tomography/computed tomography (PET/CT) is currently the standard method of imaging used to diagnose and stage many cancers and to evaluate the response to therapy. PET/CT has the advantage of providing both functional and anatomical information about diseases at the same time. Multimodality image fusion of PET and CT is clinically significant in that it permits an accurate localization of viable tumors, shown unequivocally by PET, with respect to the detailed anatomic map provided by CT. Because the fusion of PET and CT images assumes perfect registration of the two modalities, ensuring that the two studies are registered in different parts of the field of view (FOV) [1–3]. However, PET and CT systems are axially integrated and aligned in such a way that the sample can be transferred from one system gantry to the others automatically, so the two axially displaced fields of view can be mechanically aligned only to a certain degree, and the residual errors can impair sub-millimeter registrations [4]. The accuracy of registration is subject to errors due to mechanical misalignment or patient motion between sequential acquisitions. Accurate PET/CT alignment is essential to correctly interpret PET/CT exams.

In general, PET/CT systems are supplied with a special PET/CT offset procedure for initial establishment and subsequent checks of the registration of the PET and the CT fields of view [3]. Detailed data acquisition and analysis protocols for this quality control (QC) have been promulgated by the National Electrical Manufacturer's Association (NEMA), the American College of Radiology (ACR), other regulatory, advisory, and professional organizations [3–6], but most centers are not performing this QC after initial PET/CT offset establishment or they depend on engineers. Indeed, the Journal of Nuclear Medicine and the American College of Radiology guidelines recommend that such tests of multimodality image registration should be performed at least monthly or quarterly [5]. In this respect, the QC procedure for checking the accuracy of image registration should be performed periodically at the user level, so less time-consuming and less rigorous procedures for this QC need to be established.

The aim of this study is to establish an optimal QC procedure for checking the accuracy of PET/CT registration that can be performed by the user. Particularly, this study focused on phantom preparations and development of an image analysis tool. We tried to find the most practical and simplest method for checking the accuracy of PET/CT alignment by comparing and modifying the present phantoms and by using a variety of analysis methods. This study excluded registration factors related to the patient's motion and only considered the original registration error of PET/CT equipment. After we apply this method in practice, we want to establish

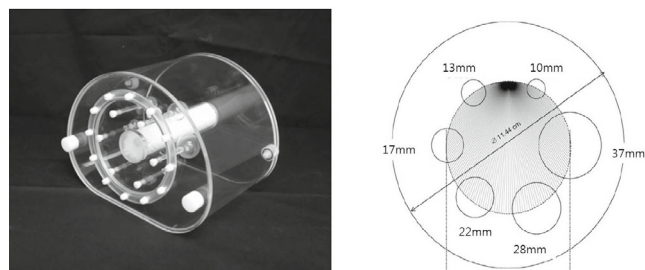


Fig. 1. NEMA IEC body phantom and view of the hollow spheres.

our guideline and suggest it to other centers.

## II. MATERIALS AND METHODS

### 1. Phantom Preparation and Positioning

Two types of phantoms were used to study the accuracy in the correlation of both imaging modalities. They are generally used to assess the image quality of PET at present. The first is NEMA International Electrotechnical Commission (IEC) phantom (Fig. 1). This phantom consists of a body phantom, a lung insert and an insert with six spheres of various diameters (10, 13, 17, 22, 28, and 37 mm). The body compartment was filled with an  $^{18}\text{F}$  solution with a 5.3 kBq/mL radioactivity concentration. The 28 and the 37 mm spheres were filled with cold water to mimic cold lesion imaging. The 10, 13, 17 and 22 mm spheres were filled with an  $^{18}\text{F}$  solution that was 8 times hotter than the background (sphere : background = 8:1), *i.e.*, with a concentration of 42.4 kBq/mL. The spheres were positioned with the centers of all the spheres in the same transverse slice at a 57.2 mm radial distance from the center of the phantom. The 17 mm sphere was positioned along the horizontal axis of the phantom. The phantom was positioned at the end of the table in a supine position. The phantom was positioned axially in the scanner so that the centers of the spheres were at the middle slice of the scanner and were positioned transaxially so that the center of the phantom was centered in the scanner [3].

The second phantom is the American College of Radiology (ACR)-approved PET phantom (Fig. 2). That phantom is a cylinder with an internal radius of 10.8 cm. The faceplate has fillable thin-walled cylinders (8, 12, 16 and 25 mm in diameter), two additional 25 mm cylinders, one for air and one for “cold” water, and a Teflon cylinder. The lower portion of the cylinder contains six sets of acrylic rods (4.8, 6.4, 7.9, 9.5, 11.1 and 12.7 mm in diameter) arranged in a pie-shaped pattern. For this study, only the faceplate parts were used. The 8, 12, 16 and 25 mm spheres were filled with an  $^{18}\text{F}$  solution that was 2.5 times hotter than the background (sphere: background = 2.5:1). The cylinders were prepared by adding

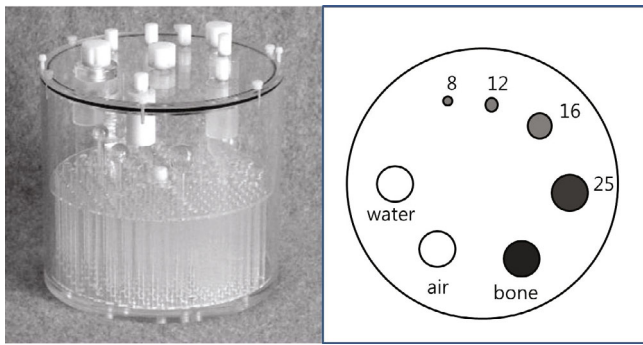


Fig. 2. ACR-approved PET phantom and faceplate view.

12.95 MBq to a 1,000 ml bag or bottle of distilled water or saline and flushing the syringe several times. The solution was mixed thoroughly. Approximately 40 ml was withdrawn for use in filling the four empty cylinders (8, 12, 16 and 25 mm) in the phantom faceplate. Two 25 mm cylinders remained, the 25 mm cylinder next to the primary extended filling cap was empty, and the neighboring 25 mm cylinder was filled with “cold” water. 12.95 MBq was injected into the phantom, and the syringe was flushed several times (phantom background activity). The solutions were thoroughly mixed [6]. The phantom was placed on the table with its flange hanging over the edge. The phantom was aligned so that it was parallel to the axis of the table.

## 2. Data Acquisition and Reconstruction

PET/CT images for both phantoms were acquired with a Biograph TruePoint 40 system (Siemens Healthcare, USA). The PET scanner is comprised by 4 rings with a total of 192 lutetium orthosilicate detectors (LSO), covering an axial FOV of 216 mm and a transaxial FOV of 70 cm in diameter; each block is  $4 \times 4 \times 20$  mm. The coincidence time window was 4.5 ns. The PET data were acquired in the 3-dimensional static mode for 2.5 min per bed position including all spheres. PET images were reconstructed with the baseline ordered-subset expectation maximization (OSEM) algorithm, the OSEM+True X model. The Biograph TruePoint 40 PET/CT scanner (Siemens Healthcare, USA) uses point spread function (PSF) modeling for improving the spatial resolution in the reconstruction, so the spatial resolution and the image quality are expected to be highly improved. There is the True X reconstruction algorithm in Siemens. The reconstruction parameters for the OSEM+True X model included 3 iterations and 21 subsets. These conditions were confirmed as optimal reconstruction parameters in terms of the spatial resolution and the image quality, so they were used in this study [7]. A Gaussian filter with a full width at half maximum (FWHM) of 3 mm was used as post-smoothing and the

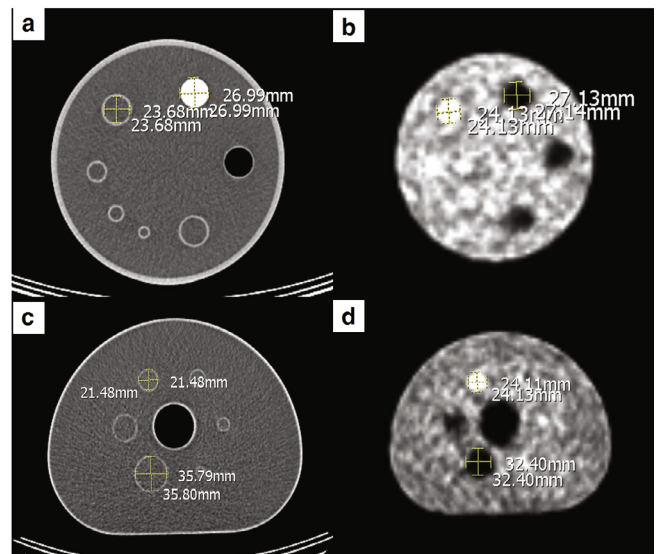


Fig. 3. (Color online) Image analysis 1 to measure the degree of alignment PET and CT alignment: The total difference between the target centers on PET and CT was measured, and the regions of interest (ROI) were set on the largest hot and cold spheres in both of the phantoms. (a) CT axial image of ACR-approved PET phantom, (b) PET axial image of ACR-approved PET phantom, (c) CT axial image of the NEMA IEC body phantom, (d) PET axial image of the NEMA IEC body phantom.

image matrix was  $168 \times 168$ , with 4.07 mm pixels. The PET image slice thickness was 5 mm. The CT scan was performed using the following parameters: 120 kV, 100 mA, 0.5 s tube rotation, and 5 mm slice thickness. The CT data were used for attenuation correction and fusion images.

## 3. Data Analysis

We analyzed the degree of alignment PET and CT using two methods. The first method was to verify correspondence on the scales on the left to right axis (x coordinate) and the anterior-to-posterior axis (y coordinate) in CT and PET axial images by using fusion image software (INFINITT Healthcare). We measured total difference between the target centers on PET and CT, the region of interest (ROI), was set on the largest hot and cold sphere in both phantoms. Distances were determined by trained technicians measured using measuring tools (ruler). On zoomed PET transverse images, the slice with the maximum area of target activity was initially found, giving the Z coordinate. Subsequently, the center of the target was obtained by triangulating on the visual determined center of the target, giving the X and the Y coordinates. The same process as that for the PET imaging was then used for CT, selecting the transaxial slice with the maximum area of the target

Table 1. Total difference between the target centers on PET and CT (ACR-approved PET phantom & NEMA IEC body phantom) [unit: mm].

ACR-approved PET phantom			
The largest hot sphere		The largest cold sphere	
CT	PET	CT	PET
X : 23.68	X : 24.13	X : 26.99	X : 27.13
Y : 23.68	Y : 23.68	Y : 23.68	Y : 23.68
Z : 5.00	Z : 5.00	Z : 5.00	Z : 5.00
$\Delta X = -0.45, \Delta Y = 0.45, \Delta Z = 0$		$\Delta X = 0.14, \Delta Y = 0.14, \Delta Z = 0$	
Difference = $\sqrt{(-0.45)^2 + (-0.45)^2}$ = $0.636 \pm 0.11$		Difference = $\sqrt{(0.14)^2 + (0.14)^2}$ = $0.198 \pm 0.09$	
NEMA IEC body phantom			
The largest hot sphere		The largest cold sphere	
CT	PET	CT	PET
X : 21.48	X : 24.11	X : 35.79	X : 32.40
Y : 21.48	Y : 24.13	Y : 35.80	Y : 32.40
Z : 5.00	Z : 5.00	Z : 5.00	Z : 5.00
$\Delta X = -2.63, \Delta Y = -2.65, \Delta Z = 0$		$\Delta X = 3.39, \Delta Y = 3.40, \Delta Z = 0$	
Difference = $\sqrt{(-2.63)^2 + (-2.65)^2}$ = $3.720 \pm 0.97$		Difference = $\sqrt{(3.39)^2 + (3.40)^2}$ = $4.800 \pm 0.85$	

density. To improve the reproducibility of the measurements, use repeated the process five times with the same trained technician. The coordinate differentials on the three axes was measured in pixels, delta X being defined as coordinate X axis PET - coordinate X axis CT; the same process was used for the Y and the Z axes. The total difference between the target centers on PET and CT was determined by using the following formula: Difference =  $(\Delta X^2 + \Delta Y^2 + \Delta Z^2)^{0.5}$  More details on this method have been given in Ref. 8 (Fig. 3).

Our second method was to measure the x location at the line profile of the target on the PET and the CT transverse images. For that, we used a medical imaging data examiner (AMIDE). AMIDE is a completely free tool for viewing, analyzing, and registering volumetric medical imaging data sets. (For help and information, see the AMIDE user's email list: amide-userslists.sourceforge.net.) We calculated the difference in the x locations at the overlapped line profiles of the PET and the CT transverse images. The ROI were set on bone, air and hot sphere in the case of the ACR-approved PET phantom and an air and the hot sphere in the case of the NEMA IEC body phantom (Fig. 4, 5). Finally, we measured the total time required for preparation of the phantom to check the practicality and usefulness of QC procedure. A technician prepared the phantom three times, and the mean  $\pm$  SD minutes were calculated.

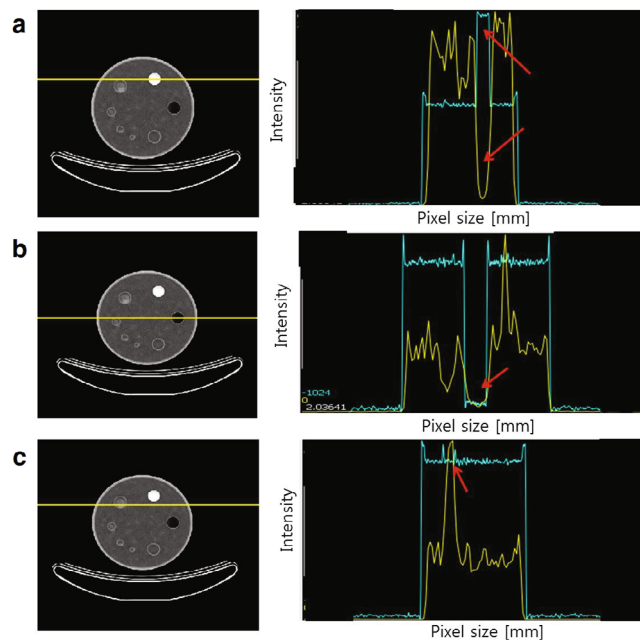


Fig. 4. (Color online) Transaxial fusion PET/CT image (left) and the line profile (right) of each ROI of ACR-approved PET phantom (green line: CT, yellow line: PET, red arrow: overlapped point): (a) bone sphere, (b) air sphere, (c) hot sphere.



Table 2. The measured x location at the line profile of the target on PET and CT [unit: mm].

target	ACR-approved PET phantom			NEMA IEC body phantom		
	Bone	Air	Hot sphere	Bone	Air	Hot sphere
CT	4.90/32.85	47.49/74.12	-66.99/41.70	N/A	-24.39/22.20	-39.03/-20.40
PET	3.57/32.52	48.75/75.45	-68.66/-43.30	N/A	-23.06/26.20	-37.70/-19.70
Difference	1.33/1.33	-1.26/1.60	-1.67/1.60	N/A	-1.33/4.00	1.33/-1.29

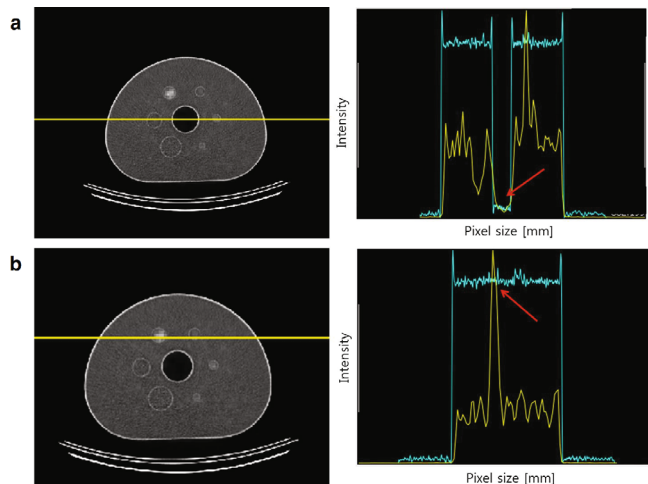


Fig. 5. (Color online) Transaxial fusion PET/CT image (left) and the line profile (right) of each ROI of the NEMA IEC body phantom (green line: CT, yellow line: PET, red arrow: overlapped point): (a) air sphere and (b) hot sphere.

### III. RESULTS

The total difference was  $0.636 \pm 0.11$  mm for the largest hot sphere and was  $0.198 \pm 0.09$  mm for the largest cold sphere in the case of the ACR-approved PET phantom (Table 1). The total difference was  $3.720 \pm 0.97$  mm for the largest hot sphere and was  $4.800 \pm 0.85$  mm for the largest cold sphere in the case of the NEMA IEC body phantom (Table 2). These values were within the acceptable range ( $\pm 5.00$  mm). The misalignment errors for the NEMA IEC body phantom were a little higher than these for ACR-approved PET phantom when the first analysis method was used. The second analysis method showed that the difference in the x location values at the line profile of the lesion on PET and CT were (1.33, 1.33) mm on the bone lesion, (-1.26, -1.33) mm on the air lesion and (-1.67, -1.60) mm on the hot sphere lesion for the ACR-approved PET phantom. For the NEMA IEC body phantom the difference in the x location values at the line profile of the lesion on PET and CT were (-1.33, 4.00) mm on the air lesion and (1.33, -1.29) mm on the hot sphere lesion (Table 3). The bone lesion for the NEMA IEC body phantom was excluded because that part was not in the phantom.

Table 3. Mean time required from phantom preparation [unit: min].

Trail	ACR-approved PET phantom	NEMA IEC body phantom
1st	72	105
2nd	68	97
3rd	63	88
mean $\pm$ SD	$67.72 \pm 4.5$	$96.78 \pm 8.5$

Similar to the first analysis method, these values are within the acceptable range ( $\pm 5.00$  mm). This method showed that the misalignment errors for the NEMA IEC body phantom were a little higher than these for the ACR-approved PET phantom. All the misalignment errors from both analysis methods were within  $\pm 5.00$  mm (this acceptable criteria is recommended by Siemens and GE manufacturer) [12,14]. We confirmed that the misalignment errors for the NEMA IEC body phantom were a little higher than these for the ACR-approved PET phantom in both methods and that variation was much higher in the first analysis method than in the second analysis method. Meanwhile, the total time required from phantom preparation was  $67.72 \pm 4.50$  min for the ACR-approved PET phantom and  $96.78 \pm 8.50$  min for the NEMA IEC body phantom. The lead time for the ACR-approved PET phantom was less than that for the NEMA IEC body phantom (Table 3).

### IV. DISCUSSION

In this study, we developed the analysis tool to check the accuracy of the PET/CT registration when using an ACR-approved PET phantom and an NEMA IEC body phantom and applied it to a clinical situation. Then, based on the results, we evaluated the usefulness of this tool. As the result of this study shows, the registration errors in both the ACR-approved PET phantom and the NEMA IEC body phantom were within the acceptable range. The registration error when using the NEMA IEC phantom was a little higher than that when using the ACR-approved PET phantom, (Table 1) because of the

variation derived from the operator in the first analysis tool. For that reason, we concluded that the method using the ACR-approved PET phantom would be more useful and practical than the method using the NEMA IEC body phantom. The lead time for preparation of the ACR-approved PET phantom was shorter than that for the preparation of the NEMA IEC body phantom (Table 3).

In general, the accuracy of registration depends on the positioning accuracy of the patient-handling system and the time between acquisitions of attenuation correction data and acquisitions of the PET data. The manufacturer measures the accuracy and reproducibility of the PET/CT patient-positioning system before introducing the product to the market [1]. For the Biograph Truepoint 40 PET/CT system used in this study, the reported positioning accuracy is less than 0.5 mm, and the positioning reproducibility is 0.5 mm. However, most centers do not perform follow-up tests routinely to check for misalignment errors that might arise while using the PET/CT scanner after the initial test; guidelines recommend for users to check it routinely. Reference 5 and 13 reported that it should be checked quarterly or monthly, and Reference 3 reported that it must be checked either after separating the PET and the CT gantries for servicing, system calibration, and software changes or upgrades or the calibration procedure should be performed once a month, as part of regular maintenance, or when a need for calibration is indicated by inspection of the daily two-bed test scan results [12]. Nowadays, nuclear medicine (NM) instruments (gamma cameras, SPECT/CT scanners, dose calibrators, survey meters, uptake probes), including PET/CT scanner, are checked daily, monthly, quarterly, and annually as well established by broad outlines. However, the accuracy of PET/CT registration QC was not included in the case of our center. There this study intended to develop a less time-consuming and less rigorous procedure because manufacturer-recommended acceptance-testing, QC, and preventive-maintenance procedures performed at initial installation are too difficult and impractical to perform for day-to-day QC. This study is valuable in autonomously developing the procedure to check the registration error of PET and CT. This study is meaningful because our method can be applied to all kinds of manufacture's PET/CT scanners, in contrast to manufacturer-recommended acceptance-testing procedures, which can be applied only to their PET/CT scanners (GE manufacturer-recommended procedures can be applied only to GE PET/CT scanners, and Siemens manufacturer recommended procedures can be applied only to GE PET/CT scanners). Our recommended method can be applied to a variety of PET/CT systems regardless of manufacturer, thus, this procedure is considered to be more practical in centers that have the PET/CT scanners from various manufacturers.

The limitations of this study are as follows: The first is the potential for imprecise localization of the hot and

the cold spheres isocenters in the first analysis method, which is subjective and operator dependent, although previous studies of PET/CT were performed with similar methods [8]. However, this will be complemented by the second analysis method. Second, we could not measure rotational errors, so we recommended using this method only for a simple check of PET/CT registration. This method will be reinforced in further research by including measurement of the rotational errors.

## V. CONCLUSION

The registration errors from this study were reasonable compared with those reported in previous studies. However, when the registration errors and the lead time are considered, the method using an ACR-approved PET phantom was more practical and useful than using a NEMA IEC body phantom. The experimental and analysis methods proposed in this study are expected to be useful for checking the accuracy of PET/CT alignment. We recommend that, based on the method of this study and other guidelines, QC procedures be established to determine the accuracy of PET/CT registration. We expect our method to be used by centers interested in quality assurance (QA) of multimodality equipment.

## ACKNOWLEDGMENTS

This study was supported by grants 2012-007883 and 2014R1A2A1A10050270 from the Mid-career Researcher Program through the National Research Foundation (NRF) funded by the Ministry of Science, ICT & Future Planning (MSIP) of Korea. This work was supported by the Industrial R&D program of Mistry of Trade, Industry and Energy (MOTIE) / Korea Evaluation Institute of Industrial Technology (KEIT) (10048997; Development of the core technology for integrated therapy devices based on real-time MRI-guided tumor tracking), this research was also supported by a grant from the Korea Health Technology R&D Project through the Korea Health Industry Development Institute (KHIDI) funded by the Ministry of Health & Welfare, Republic of Korea (grant number: HI14C1135). And, this research was supported by a grant of The Catholic University of Korea-Sogang University Joint Research Project [B0001-00015, Development of MR-Ultrasound guided High Intensity Focused Ultrasound treatment system].

## REFERENCES

- [1] R. Rakheja, L. DeMello and H. Chandarana, *Ame. J. Roentgen.* **201**, 1120 (2013).

- [2] R. Shekhar, V. Walimbe and S. Raja, *J. Nucl. Med.* **46**, 1488 (2005).
- [3] G. El Fakhri, R. Fulton and J. E. Gray, *Quality assurance for PET and PET/CT systems* (IAEA, Vienna, 2009), p. 40.
- [4] A. Rodríguez-Ruano, J. Pascau and J. Chamorro, 2008 IEEE Nuclear Science Symposium Conference Record (Madrid, Spain, November 14, 2008), p. 3832.
- [5] P. Zanzonico, *J. Nucl. Med.* **49**, 1114 (2008).
- [6] ACR, *PET phantom instructions for evaluation of PET image quality* (ACR, USA, 2006), p. 3.
- [7] Y. S. Lee, J. S. Kim and K. M. Kim, *Ann. Nucl. Med.* **28**, 340 (2014).
- [8] C. Cohade, M. Osman and L. T. Marshall, *Eur. J. Nucl. Med. Imaging* **30**, 721 (2003).
- [9] T. Chang, G. Chang and J. W. Clark, *Med. Phys.* **39**, 5891 (2012).
- [10] M. C. Baños-Capilla, M. A. García and J. Bea, *Med. Phys.* **34**, 1911 (2007).
- [11] G. Akamatsu, K. Ishikawa and K. Mitsumoto, *J. Nucl. Med.* **53**, 1716 (2012).
- [12] CPI Innovations, *ECAT LSO PET/CT 16 with PICO 3D Operator's Guide* (CPS Innovations, Tennessee, USA, 2003).
- [13] E. B. Sokole, A. Płachcińska and A. Britten, *Eur. J. Nucl. Med. Imaging* **37**, 662 (2010).
- [14] General Electric Company, *Optima 560, Discovery 600, 690 Elite PET/CT Service Manual* (GE Healthcare, USA, 2013), p. 134.
- [15] L. Sing, *Int. J. Radiat. Oncol. Biol. Phys.* **71**, S38 (2008).
- [16] A. Isambert, G. Bonniaud and F. Lavielle, *Cancer/Radiotherapie* **12**, 800 (2008).
- [17] M. Sharpe and K. K. Brock, *Int. J. Radiation Oncology Biol. Phys.* **71**, S33 (2008).
- [18] Y. Watanabe and E. Y. Han, *J. Neurosurg.* **109**, 21 (2008).
- [19] W. V. Vogela, J. A. van Dalena and D. A. X. Schinagl, *Nucl. Med. Commun.* **27**, 515 (2006).
- [20] K. J. Nichols, S. L. Bacharach and S. R. Bergmann, *J. Nucl. Cardiol.* **13**, e25 (2006).
- [21] A. H. Ng, K. H. Ng and H. Dharmendra, *App. Rad. and Isotop.* **67**, 1864 (2009).